



Cite this: *Chem. Commun.*, 2016, 52, 11689

Received 31st July 2016,
Accepted 31st August 2016

DOI: 10.1039/c6cc06332b

www.rsc.org/chemcomm

A supramolecular pyrenyl glycoside-coated 2D MoS₂ composite electrode for selective cell capture†

Mokhtari Wahiba,^a Xue-Qing Feng,^a Yi Zang,^b Tony D. James,^c Jia Li,^{*a} Guo-Rong Chen^a and Xiao-Peng He^{*a}

Here we demonstrate the simple construction and characterization of a pyrenyl glycoside-coated 2D MoS₂ material composite capable of selectively capturing proteins and live cells on an electrode, as determined by differential pulse voltammetry.

The ability to selectively capture a target cell on a solid support is important for the advancement of cell biology and clinical diagnosis. Many bioinspired, well-defined material surfaces are developed, for which bioselectivity relies on unique topological features directed towards specific cell morphologies.¹ However, to isolate a cell on the surface, immunosorbent assays that depend on the capture of a cell-surface biomarker by monoclonal antibodies are required. But, the preparation of antibodies is sluggish and costly, and the conventional immunosorbent protocols are accompanied by high technical demand and long detection time. As a result, simpler and more effective methods for selective cell capture are urgently required.

Receptor–ligand interactions are crucial for a number of physiological and pathological events. These interactions are selective and have been shown to be applicable for targeted cell imaging and drug delivery.^{2–6} The coating of ligand arrays onto material surfaces has resulted in effective sensing systems for the selective detection of biomacromolecules and cells/pathogens that express receptors for the attached ligands.^{7,8} These advanced sensors could be an alternative to traditional immunoassays. Of the many smart sensing systems developed, the construction of 2D graphene composite electroensors has been of particular interest because of the ease and flexibility in sensor fabrication, high sensitivity and short detection time.^{9–12} Recently, increasing

efforts have been made in the development of 2D graphene analogues (for example 2D transition metal dichalcogenides [TMDs]) as multifunctional materials.^{13,14} These materials have also found application in biosensing and disease theranostics.^{15–20} With continuing interest in the development of functional 2D composite materials,^{21–26} here we illustrate the use of 2D TMD for the simple construction of a composite electrode that selectively captures a target cell over other control cells.

A glycoligand (galactose) that is selectively recognized by a cell-surface galactose receptor (the asialoglycoprotein receptor [ASGPR])²⁷ was used to couple with a binder to the 2D material surface. Pyrene was used as the binder for surface attachment due to its planarity.⁶ Click chemistry²⁸ coupling of the glycoligand with a polyethylene glycol (PEG)-grafted pyrene-1-butyric acid produced the glycopyrene (**WXB**) (Fig. 1a and Scheme 1). The 2D MoS₂ sheets were prepared by a liquid exfoliation method.²⁹ Subsequently, the components (**WXB** and 2D MoS₂) were mixed in an aqueous solution (Tris-HCl, 0.01 M, pH 7.4) and sonicated for 1 h to facilitate assembly. The formation of the supramolecular **WXB**/2D MoS₂ composite is probably driven by the van der Waals interactions between **WXB** and 2D MoS₂.³⁰

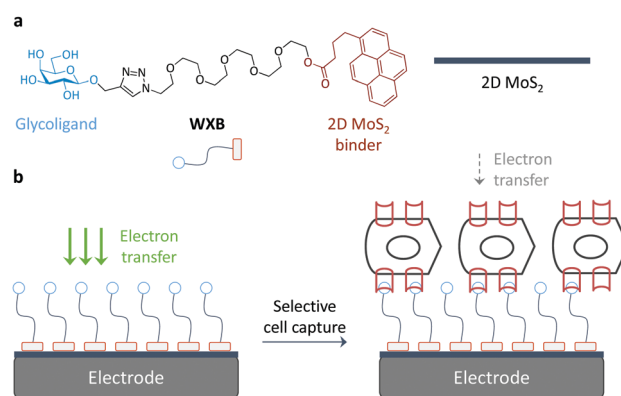


Fig. 1 (a) Structure of pyrenyl galactoside (**WXB**) and (b) schematic illustration of the 2D MoS₂ composite electrode for selective cell capture.

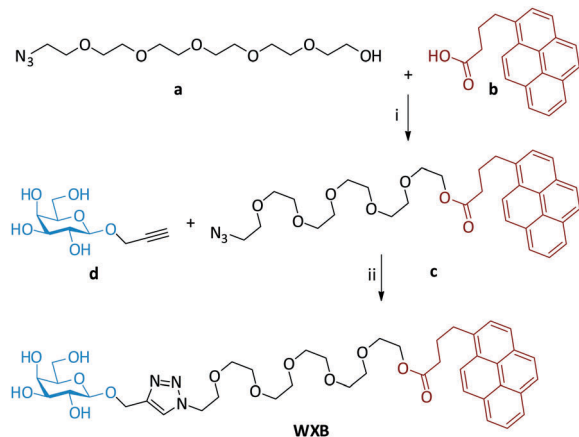
^a Key Laboratory for Advanced Materials & Institute of Fine Chemicals, East China University of Science and Technology, 130 Meilong Rd., Shanghai 200237, P. R. China. E-mail: xphe@ecust.edu.cn

^b National Center for Drug Screening, State Key Laboratory of Drug Research, Shanghai Institute of Materia Medica, Chinese Academy of Sciences, 189 Guo Shoujing Rd., Shanghai 201203, P. R. China. E-mail: jli@simm.ac.cn

^c Department of Chemistry, University of Bath, Bath, BA2 7AY, UK

† Electronic supplementary information (ESI) available: Additional figures and experimental section. See DOI: 10.1039/c6cc06332b





Scheme 1 Reagents and conditions: (i) EDC-HCl and DMAP in CH_2Cl_2 ; (ii) $\text{CuSO}_4 \cdot 5\text{H}_2\text{O}$, Na ascorbate in $\text{CH}_2\text{Cl}_2/\text{TBA}/\text{H}_2\text{O}$.

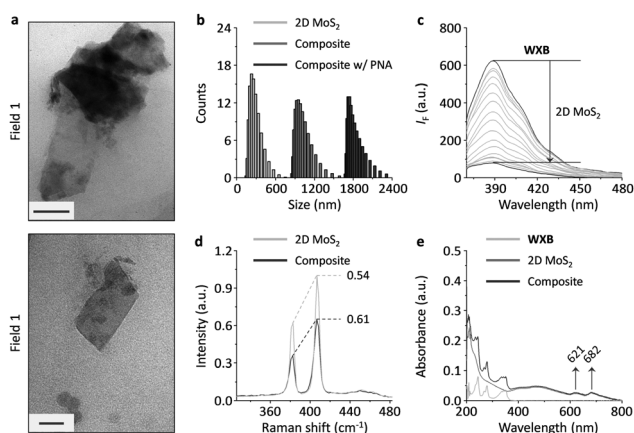


Fig. 2 (a) Transmission electron microscopy of 2D MoS_2 (scale bars: field 1 = 50 nm; field 2 = 100 nm). (b) Dynamic light scattering of 2D MoS_2 ($50 \mu\text{g mL}^{-1}$), composite ($\text{WXB}/2\text{D MoS}_2 = 0.5 \mu\text{M}/50 \mu\text{g mL}^{-1}$) and the composite with peanut agglutinin (PNA, $1.5 \mu\text{M}$). (c) Fluorescence titration of **WXB** ($1 \mu\text{M}$) in the presence of increasing 2D MoS_2 (0 – $20 \mu\text{g mL}^{-1}$) in Tris-HCl (0.01 M , pH 7.4) with an excitation at 349 nm. (d) Raman spectroscopy of 2D MoS_2 ($100 \mu\text{g mL}^{-1}$) and composite ($\text{WXB}/2\text{D MoS}_2 = 10 \mu\text{M}/100 \mu\text{g mL}^{-1}$). (e) UV-vis spectroscopy of **WXB** ($2 \mu\text{M}$), 2D MoS_2 ($20 \mu\text{g mL}^{-1}$) and composite ($\text{WXB}/2\text{D MoS}_2 = 2 \mu\text{M}/20 \mu\text{g mL}^{-1}$).

To characterize the material, a variety of techniques were employed. Objects shown in the transmission electron microscopy images of 2D MoS_2 appeared to be thin layers (Fig. 2a), suggesting the existence of the 2D material.²⁹ Dynamic light scattering (DLS) indicated that the particle size of 2D MoS_2 was in the range of 70–400 nm (Fig. 2b).²⁹ While the composite showed an increased size distribution with respect to 2D MoS_2 , the subsequent addition of a galactose-selective lectin (peanut agglutinin [PNA]) further increased the size. This suggests that the 2D composite could interact with a selective protein receptor to form a larger biomatrix. The fluorescence of **WXB** (pyrene fluorescence) was quenched in a concentration-dependent manner by 2D MoS_2 (Fig. 2c). This is in agreement with the quenching property of the 2D material for closely attached fluorescent species.^{13–15} The quantum yields of **WXB** in water

before and after assembly with 2D MoS_2 were determined to be 0.15 and 0.03, respectively.

Typical Raman shifts of 2D MoS_2 were observed at ca. 405 and 383 cm^{-1} , which are assigned to the out-of-plane vibration of S (A_{1g}) and in-plane relative motion between S and Mo (E_{2g}^1) modes of the MoS_2 crystal (Fig. 2d).³¹ We observed that the E_{2g}^1/A_{1g} ratio of the composite increased with respect to that of 2D MoS_2 alone, suggesting a perturbation towards the in-plane relative motion between S and Mo by the molecular coating.³² In addition, typical UV shifts (621 and 682 nm, which are ascribed to the A1 and B1 direct exciton transitions of 2D MoS_2 , respectively) were observed for both 2D MoS_2 and the composite (Fig. 2e).³¹ These data suggest the successful formation of the pyrenyl glycoside-coated 2D MoS_2 composite.

With the composite in hand, we then tested its ability to capture cells on an electrode surface (Fig. 1b). Our previously developed screen-printed electrode (SPE) was used.^{6,33} To the working electrode area, 2D MoS_2 and pyrenyl glycoside were dripped sequentially, forming a supramolecular composite on the surface. On the basis of the DLS result that the composite might interact selectively with specific lectins, we used differential pulse voltammetry (DPV) to measure the recognition using $[\text{Fe}(\text{CN})_6]^{3-/4-}$ as a redox probe.³⁴

We observed the typical DPV signal of the redox probe, which was gradually decreased with increasing PNA, a galactose-selective lectin (Fig. 3a). The quenched signal could be reasoned by the adhesion of the protein onto the glycoside layer of the composite electrode, thereby compromising electron transfer (Fig. 1b).^{33–35} A good linearity was observed over a wide PNA concentration range (Fig. 3b), and the limit of detection (LOD) for the electrode

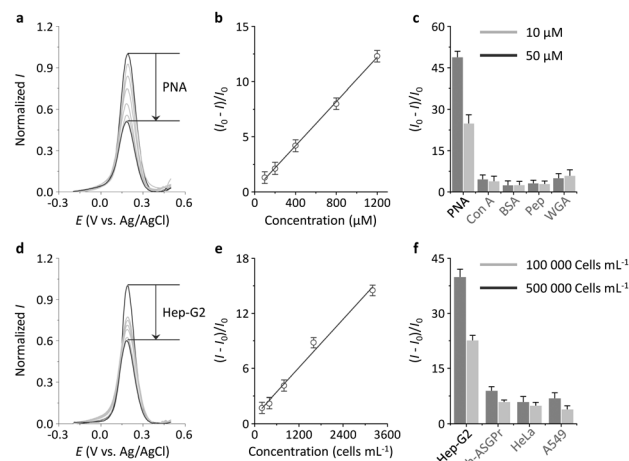


Fig. 3 Differential pulse voltammetry of the 2D MoS_2 composite electrode (with 5 mM of $[\text{Fe}(\text{CN})_6]^{3-/4-}$) with (a) increasing peanut agglutinin (PNA, 0–50 μM) and (d) increasing Hep-G2 (human hepatoma) cells (0–500 000 cells mL^{-1}). Plotting the current intensity decrease of the electrode as a function of (b) PNA concentration and (e) Hep-G2 cell concentration, where I and I_0 are the current intensity of $[\text{Fe}(\text{CN})_6]^{3-/4-}$ in the presence and absence of an analyte, respectively. Current intensity change of electro-sensors in the presence of (c) different proteins (Con A = concanavalin A; BSA = bovine serum albumin; Pep = pepsin; WGA = wheat germ agglutinin) and (f) different cells (sh-ASGPr = Hep-G2 with reduced ASGPr expression; HeLa = human cervical cancer cells; A549 = human lung cancer cells).



towards PNA was determined to be 373 nM. A selectivity test showed that the current decrease of the redox probe was specific for the selective lectin (PNA), over other non-selective proteins including the mannose-selective concanavalin A, the *N*-acetyl glucosamine-selective wheat germ agglutinin, bovine serum albumin and pepsin (Fig. 3c and Fig. S1, ESI[†]). With these promising outcomes in hand we set out to evaluate cell capture using the composite electrode.

A hepatoma cell line that highly expresses ASGPr, which is selective for galactose, was used. An established sh-ASGPr cell line²¹ with a reduced receptor expression level and two other cells HeLa (human cervical cancer) and A549 (human lung cancer) without ASGPr expression were used as controls.^{36–39} We determined a concentration-dependent current decrease of the composite electrode towards Hep-G2 (Fig. 3d). A linear relationship was observed over a cellular concentration range; the LOD for the electrode towards the cells was determined to be 840 cells mL⁻¹ (Fig. 3e). Interestingly, the current signal change was hardly observed for all the control cells with reduced or without receptor expression (Fig. 3f and Fig. S2, ESI[†]). In addition, the incubation of a mixed cell culture of Hep-G2 and HeLa did not alter the sensitivity of the electrode to Hep-G2 cells (Fig. S3, ESI[†]). These pieces of evidence suggest the good biospecificity of our 2D composite system for cell capture in a receptor-targeting manner.

In order to test the reversibility of the composite, a useful attribute for the isolation of captured cells, we carried out competition assays. Thus, we determined that preincubation with increasing concentrations of free D-galactose and **WXB** with Hep-G2 caused a gradual current increase of the electrode (Fig. S4, ESI[†]), implying that the receptor-mediated capture of cells is reversible. We also used electrochemical impedance spectroscopy to investigate both protein and cell capture. Nyquist plots of the 2D composite electrode in the presence of increasing PNA and Hep-G2 cells (Fig. S5, ESI[†]) show increasing capacitive loops with added analytes suggesting a gradual increase in electron-transfer resistance of the composite electrode. Clearly indicating a coating of proteins/cells on the electrode surface as a result of ligand–receptor recognition.⁴⁰

In summary, we have demonstrated that a simple 2D MoS₂ based pyrenyl^{41,42} glycomposite material can be used for the selective capture of cells on an electrode surface. This research may help the development of 2D-material composite based sensors for solid-phase analysis of cells and disease diagnostics.^{43–50}

This research was supported by the 973 project (2013CB733700), the Science and Technology Commission of Shanghai Municipality (15540723800), the National Natural Science Foundation of China (21572058, 21576088 and 81302820) and the Shanghai Rising-Star Program (16QA1401400) (X.-P. H.). The Catalysis and Sensing for our Environment (CASE) network is thanked for research exchange opportunities. T. D. J. thanks ECUST for a guest professorship.

Notes and references

- X. Liu and S. Wang, *Chem. Soc. Rev.*, 2014, **43**, 2385.
- E. I. Rigopoulou, D. Roggenbuck, D. S. Smyk, C. Liaskos, M. G. Mythilinaiou, E. Feist, K. Conrad and D. P. Bogdanos, *Autoimmun. Rev.*, 2012, **12**, 260.
- K. Jain, P. Kesharwani, U. Gupta and N. K. Jain, *Biomaterials*, 2012, **33**, 4166.
- H.-L. Zhang, X.-L. Wei, Y. Zang, J.-Y. Cao, S. Liu, X.-P. He, Q. Chen, Y.-T. Long, J. Li, G.-R. Chen and K. Chen, *Adv. Mater.*, 2013, **25**, 4097.
- W. Ma, H.-T. Liu, X.-P. He, Y. Zang, J. Li, G.-R. Chen, H. Tian and Y.-T. Long, *Anal. Chem.*, 2014, **86**, 5502.
- X.-P. He, B.-W. Zhu, Y. Zang, J. Li, G.-R. Chen, H. Tian and Y.-T. Long, *Chem. Sci.*, 2015, **6**, 1996.
- X.-P. He, Y. Zang, T. D. James, J. Li and G.-R. Chen, *Chem. Soc. Rev.*, 2015, **44**, 4239.
- E. Paleček, J. Tkáč, M. Bartošik, T. Bertók, V. Ostatná and J. Paleček, *Chem. Rev.*, 2015, **115**, 2045.
- D. Chen, H. Feng and J. Li, *Chem. Rev.*, 2012, **112**, 6027.
- X. Huang, Z. Zeng, Z. Fan, J. Liu and H. Zhang, *Adv. Mater.*, 2012, **24**, 5979.
- X. Yu, K. Sheng, J. Chen, C. Li and G. Shi, *Acta Chim. Sin.*, 2014, **72**, 319.
- A. Ambrosi, C. K. Chua, N. M. Latiff, A. H. Loo, C. H. A. Wong, A. Y. S. Eng, A. Bonanni and M. Pumera, *Chem. Soc. Rev.*, 2016, **45**, 2458.
- M. Pumera and A. H. Loo, *Trends Anal. Chem.*, 2014, **61**, 49.
- Y. Chen, C. Tan, H. Zhang and L. Wang, *Chem. Soc. Rev.*, 2015, **44**, 2681.
- C. Zhu, Z. Zeng, H. Li, F. Li, C. Fan and H. Zhang, *J. Am. Chem. Soc.*, 2013, **135**, 5998.
- Y. Zhang, B. Zheng, C. Zhu, X. Zhang, C. Tan, H. Li, B. Chen, J. Yang, J. Chen, Y. Huang, L. Wang and H. Zhang, *Adv. Mater.*, 2015, **27**, 935.
- H. Fan, Z. Zhao, G. Yan, X. Zhang, C. Yang, H. Meng, Z. Chen, H. Liu and W. Tan, *Angew. Chem., Int. Ed.*, 2015, **54**, 4801.
- L. Cheng, J. Liu, X. Gu, H. Gong, X. Shi, T. Liu, C. Wang, X. Wang, G. Liu, H. Xing, W. Bu, B. Sun and Z. Liu, *Adv. Mater.*, 2014, **26**, 1886.
- T. Liu, C. Wang, X. Gu, H. Gong, L. Cheng, X. Shi, L. Feng, B. Sun and Z. Liu, *Adv. Mater.*, 2014, **26**, 3433.
- S. S. Chou, B. Kaehr, J. Kim, B. M. Foley, M. De, P. E. Hopkins, J. Huang, C. J. Brinker and V. P. Dravid, *Angew. Chem., Int. Ed.*, 2013, **52**, 4160.
- (a) X. Sun, B. Zhu, D.-K. Ji, Q. Chen, X.-P. He, G.-R. Chen and T. D. James, *ACS Appl. Mater. Interfaces*, 2014, **6**, 10078; (b) X.-P. He, Q. Deng, L. Cai, C.-Z. Wang, Y. Zang, J. Li, G.-R. Chen and H. Tian, *ACS Appl. Mater. Interfaces*, 2014, **6**, 5379.
- D.-K. Ji, G.-R. Chen, X.-P. He and H. Tian, *Adv. Funct. Mater.*, 2015, **25**, 3483.
- D.-K. Ji, Y. Zhang, X.-P. He and G.-R. Chen, *J. Mater. Chem. B*, 2015, **3**, 6656.
- D.-K. Ji, Y. Zhang, Y. Zang, W. Liu, X. Zhang, J. Li, G.-R. Chen, T. D. James and X.-P. He, *J. Mater. Chem. B*, 2015, **3**, 9182.
- D. Xie, D.-K. Ji, Y. Zhang, J. Cao, H. Zheng, L. Liu, Y. Zang, J. Li, G.-R. Chen, T. D. James and X.-P. He, *Chem. Commun.*, 2016, **52**, 9418.
- X.-P. He and H. Tian, *Small*, 2016, **12**, 144.
- J. B. Burgess, J. U. Baenziger and W. R. Brown, *Hepatology*, 1992, **15**, 702–706.
- X.-P. He, Y.-L. Zeng, Y. Zang, J. Li, R. A. Field and G.-R. Chen, *Carbohydr. Res.*, 2016, **429**, 1.
- J. N. Coleman, M. Lotya, A. O'Neill, S. D. Bergin, P. J. King, K. Young, A. Gaucher, S. De, R. J. Smith, I. V. Shvets, S. K. Arora, G. Stanton, H.-Y. Kim, K. Lee, G. T. Kim, G. S. Duesberg, T. Hallam, J. J. Boland, J. J. Wang, J. F. Donegan, J. C. Grunlan, G. Moriarty, A. Shmeliov, R. J. Nicholls, J. M. Perkins, E. M. Grievson, K. Theuwissen, D. W. McComb, P. D. Nellist and V. Nicolosi, *Science*, 2011, **311**, 568.
- C. Zhu, Z. Zeng, H. Li, F. Li, C. Fan and H. Zhang, *J. Am. Chem. Soc.*, 2013, **135**, 5998.
- C. Lee, H. Yan, L. E. Brus, T. F. Heinz, J. Hone and S. Ryu, *ACS Nano*, 2010, **4**, 2695–2700.
- P. T. K. Loan, W. Zhang, C.-T. Lin, K.-H. Wei, L.-J. Li and C.-H. Chen, *Adv. Mater.*, 2014, **26**, 4838.
- Z. Li, S.-S. Deng, Y. Zang, Z. Gu, X.-P. He, G.-R. Chen, K. Chen, T. D. James, J. Li and Y.-T. Long, *Sci. Rep.*, 2013, **3**, 2293.
- L. Cui, B.-W. Zhu, S. Qu, X.-P. He and G.-R. Chen, *Dyes Pigm.*, 2015, **121**, 312.
- X.-P. He, X.-W. Wang, X.-P. Jin, H. Zhou, X.-X. Shi, G.-R. Chen and Y.-T. Long, *J. Am. Chem. Soc.*, 2011, **133**, 3649.
- X.-L. Hu, Y. Zang, J. Li, G.-R. Chen, T. D. James, X.-P. He and H. Tian, *Chem. Sci.*, 2016, **7**, 4004.



- 37 K.-B. Li, Y. Zang, H. Wang, J. Li, G.-R. Chen, T. D. James, X.-P. He and H. Tian, *Chem. Commun.*, 2014, **50**, 11735.
- 38 L. Dong, Y. Zang, D. Zhou, X.-P. He, G.-R. Chen, T. D. James and J. Li, *Chem. Commun.*, 2015, **51**, 11852.
- 39 D.-T. Shi, D. Zhou, Y. Zang, J. Li, G.-R. Chen, T. D. James, X.-P. He and H. Tian, *Chem. Commun.*, 2015, **51**, 3653.
- 40 E. Katz and I. Willner, *Electroanalysis*, 2003, **15**, 913.
- 41 E. Katz, *J. Electroanal. Chem.*, 1994, **365**, 157.
- 42 E. Katz, *J. Electroanal. Chem.*, 1993, **361**, 109.
- 43 T. Bertók, J. Katrík, P. Gemeiner and J. Tkac, *Microchim. Acta*, 2013, **180**, 1–13.
- 44 Y. Zhang, S. Luo, Y. Tang, L. Yu, K.-Y. Hou, J.-P. Cheng, X. Zeng and P. G. Wang, *Anal. Chem.*, 2006, **78**, 2001–2008.
- 45 S. Szunerits, J. Niedziłka-Jösön, R. Boukherroub, P. Woisel, J.-S. Baumann and A. Siriwardena, *Anal. Chem.*, 2010, **82**, 8203–8210.
- 46 O. A. Loaiza, P. J. Lamas-Ardiasana, E. Jubete, E. Ochoteco, I. Loinaz, G. Cabañero, I. García and S. Penadés, *Anal. Chem.*, 2011, **83**, 2987–2995.
- 47 A. Poghossian, E. Katz and M. J. Schöning, *Chem. Commun.*, 2015, **51**, 6564.
- 48 S. M. Silva, R. Tavalalaie, L. Sandiford, R. D. Tilley and J. J. Gooding, *Chem. Commun.*, 2016, **52**, 7528.
- 49 L. J. Raftery, Y. S. Grewal, C. B. Howard, M. L. Jones, M. J. A. Shiddiky, L. G. Carrascosa, K. J. Thurecht, S. M. Mahler and M. Trau, *Chem. Commun.*, 2016, **52**, 5730.
- 50 A. Hushegyi, T. Bertók, P. Damborsky, J. Katrík and J. Tkac, *Chem. Commun.*, 2015, **51**, 7474.

